Relativistic analyses of quasielastic neutrino cross sections at MiniBooNE kinematics

Relativistic analyses of quasielastic neutrino cross sections at MiniBooNE kinematics

J. E. Amaro,[1] M. B. Barbaro,[2] J. A. Caballero,[3] T. W. Donnelly,[4] and J. M. Udías[5]

[1]*Departamento de Física Atómica, Molecular y Nuclear, Universidad de Granada, 18071 Granada, Spain*
[2]*Dipartimento di Fisica Teorica, Università di Torino and INFN, Sezione di Torino, Via P. Giuria 1, 10125 Torino, Italy*
[3]*Departamento de Física Atómica, Molecular y Nuclear, Universidad de Sevilla, 41080 Sevilla, Spain*
[4]*Center for Theoretical Physics, Laboratory for Nuclear Science and Department of Physics, Massachusetts Institute of Technology, Cambridge, Massachusetts 02139, USA*
[5]*Grupo de Física Nuclear, Departamento de Física Atómica, Molecular y Nuclear, Universidad Complutense de Madrid, 28040 Madrid, Spain*

(Received 13 June 2011; published 8 August 2011)

Two relativistic approaches are considered to evaluate the quasielastic double-differential and integrated neutrino-nucleus cross sections. One, based on the relativistic impulse approximation, relies on the microscopic description of nuclear dynamics using relativistic mean field theory, and incorporates a description of the final-state interactions. The second is based on the superscaling behavior exhibited by electron scattering data and its applicability, due to the universal character of the scaling function, to the analysis of neutrino scattering reactions. The role played by the vector meson-exchange currents in the two-particle two-hole sector is also incorporated and the results obtained are compared with the recent data for neutrinos measured by the MiniBooNE Collaboration.

DOI: 10.1103/PhysRevD.84.033004 PACS numbers: 25.30.Pt, 13.15.+g, 24.10.Jv

I. INTRODUCTION

The data on muon neutrino charged-current quasielastic (CCQE) cross sections recently obtained by the MiniBooNE Collaboration [1], and its comparison with several theoretical calculations, have led to an important debate concerning the role played by various ingredients entering in the description of the reaction: nuclear dynamics [final-state interactions (FSI), low-lying nuclear excitations, effects beyond the impulse approximation (IA), etc.], as well as possible modifications of the single-nucleon form factors. Although no definitive conclusions are yet in hand, a detailed study of modeling versus experiment for inclusive quasielastic electron scattering and its extension to neutrino processes can shed light on the different interpretations of the discrepancy between theory and experiment.

When a dipole shape is assumed for the axial form factor, the nucleon axial mass M_A can be considered to be the only free parameter within the relativistic Fermi gas (RFG) model, presently used in many Monte Carlo codes employed in the analysis of the experimental data. When compared with MiniBoone CCQE data, the RFG underestimates the total cross section unless an axial mass M_A of the order of 1.35 GeV/c^2 is employed in the dipole prescription for the form factor. This value of the axial mass is considerably larger than the accepted world average value $M_A = 1.026 \pm 0.021$ GeV/c^2 [2], thus yielding a larger axial form factor. This should be taken more as an indication of incompleteness of the theoretical description of the MiniBooNE data based upon the RFG, rather than as a true indication for a larger axial mass.

For instance, although the RFG incorporates a fully relativistic treatment, required by the kinematics of the experiment (mean neutrino energy flux, $\langle E_\nu \rangle = 788$ MeV, with values up to 3 GeV), its description of the nuclear dynamics is clearly too crude to draw specific conclusions on the value of the anomalous axial mass from the departure of the RFG from experiment, but rather be taken as a hint on the importance of nuclear effects in describing these experimental data.

However, at the level of the impulse approximation, a number of much more sophisticated descriptions of the nuclear dynamics other than the one represented by the RFG, based, for instance, on the use of realistic spectral functions [3–5], when compared with the MiniBooNE experimental data also underpredict the measured CCQE cross section, in this respect not doing a better job than the RFG. One important consideration that must be taken into account is the fact that, even when these models provide a much more realistic description of the nuclear dynamics than the RFG, they are built on nonrelativistic approaches that are likely questionable at the kinematics of the MiniBooNE experiment.

Among the difficulties that one faces when comparing models, is that the effect of the ingredients in the model, such as interactions in the final state, may differ greatly from model to model. For example in [4] the FSI are barely seen, causing only a simple $\sim$10 MeV shift of the QE peak. However, relativistic and semirelativistic models of inclusive QE (e, e') reactions that included a relativistic mean field, that is, described the FSI by means of strong relativistic potentials or their semirelativistic equivalents, have clearly shown the essential role played by FSI in order to describe properly the behavior of data [6–10].

In addition to the relativistic treatment of the nuclear excitations, in some regions of the wide range of neutrino

energies where the neutrino flux for the experiment has significant strength, the reaction may have sizable contributions from effects beyond the IA. For instance, in [11,12] when the theoretical results incorporated multiple knock-out excitations, they were shown to be in accordance with the total cross section data without the need to increase the value of M_A. However, no comparison with the experimental double-differential cross section is shown in [11,12]. Moreover, these calculations are based on nonrelativistic reductions whose reliability at MiniBooNE kinematics may be doubtful. In fact, the kinematics of the MiniBooNE experiment demands relativity as an essential ingredient; not only relativistic kinematics should be considered, but also the nuclear dynamics and current operators should be described within a relativistic framework [13–15]. Furthermore, the wide range of neutrino energies, at least for some specific conditions, may also require one to account for effects not included in models devised for quasifree scattering. This is, for instance, the situation at the most forward scattering angles where a very significant contribution in the cross section may come from very low-lying excitations in nuclei [16].

A systematic analysis of the world inclusive (e, e') data has clearly demonstrated that, for sufficiently large momentum transfers, at energy transfers below the QE peak the property of superscaling works rather well [17–20], that is, the reduced cross section, when represented versus the scaling variable [21], is largely independent of the momentum transfer (first-kind scaling) and of the nuclear target (second-kind scaling). Moreover, from the longitudinal response a phenomenological scaling function has been extracted that shows a clear asymmetry with respect to the quasielastic peak (QEP) with a long tail extended to positive values of the scaling variable (larger energy transfers). Assuming the scaling function to be universal, i.e. , valid for electromagnetic and weak interactions, in [22,23] CCQE neutrino-nucleus cross sections were evaluated by using the scaling function extracted from (e, e') data and multiplying it by the corresponding elementary weak cross section. This approach, denoted simply as ''SuSA,'' provides nuclear-model-independent neutrino-nucleus cross sections, but its reliability rests on a basic assumption: the scaling function [extracted from longitudinal (e, e') data] is appropriate for all of the various weak responses involved in neutrino scattering (charge-charge, charge-longitudinal, longitudinal-longitudinal, transverse and axial), and is independent of the vector or axial nature of the nuclear current entering the hadronic tensor. In particular, the SuSA approach assumes the electromagnetic longitudinal (L) and transverse (T) scaling functions to be equal. This property, known as scaling of the zeroth kind, is fulfilled by the RFG (by construction) and by most models based on nonrelativistic descriptions that, in a way, factorize the elementary lepton-nucleus amplitude into a lepton-nucleon part and a part containing the nuclear effects [24,25]. Within SuSA, this factorization in the elementary amplitude propagates even to the cross section, which is then proportional to the elementary lepton-nucleon cross section and to the nuclear response, the latter in this approach being a universal function.

However, from the analysis of the existing L/T separated data, after removing inelastic contributions and two-particle-emission effects one finds that the ''purely nucleonic'' transverse scaling function is significantly larger than the longitudinal one [26]. This has to be attributed to a breakdown of the elementary factorization mentioned before, so that the elementary lepton-nucleon vertex inside the nucleus is no longer accurately described by the one for free nucleons. One must resort to models such as the relativistic mean field approach, denoted as RMF, where the relativistic dynamics introduces significant deviations of the behavior of the elementary lepton-nucleon vertex in the presence of strong scalar and vector potentials [24]. This breakdown of zeroth-kind scaling present in the RMF seems to be favored by the comparison with data [26].

In a recent paper [16] SuSA predictions have been compared with the MiniBooNE data for the double-differential neutrino cross section showing a systematic discrepancy between theory and experiment. Inclusion of $2p$-$2h$ meson-exchange current (MEC) contributions yields larger cross sections and accordingly better agreement with the data. However, this theory still lies below the data at larger angles where the cross sections are smaller. Before drawing definitive conclusions on the anomalous axial mass, it is important to explore alternative approaches that have been shown to be successful in describing inclusive QE (e, e') processes. As just mentioned, this is the case for the RMF, where a fully relativistic description (kinematics and dynamics) of the process is incorporated, and FSI are taken into account by using the same relativistic scalar and vector energy-independent potentials considered in the description of the initial bound states. The RMF model applied to inclusive QE (e, e') processes has been shown to describe scaling behavior, and more importantly, it gives rise to a superscaling function with a significant asymmetry, namely, in complete accord with data [7,27]. Moreover, contrary to SuSA, where scaling of the zeroth kind is assumed, the RMF model provides longitudinal and transverse scaling functions which differ by typically 20%, the T one being larger.

The RMF approach has been applied to the description of CCQE neutrino-nucleus cross sections [6,28–30] and it has been investigated with respect to how scaling emerges from neutrino reactions, and how the ''*theoretical*'' neutrino scaling functions compare with the corresponding ones evaluated for electrons (L and T responses) and with the data [29,30].

Even at the level of the impulse approximation, the zeroth-kind scaling violation introduced by the RMF

approach, as well as the different isospin character shown by the electromagnetic and weak nucleon form factors, can lead to significant discrepancies between the results provided by SuSA and RMF approaches. Furthermore, effects beyond the IA give rise to additional scaling violations in the transverse responses. Thus, a proper relativistic description of these effects is needed in order to compare with the data taken by the MiniBooNE Collaboration.

The paper is organized as follows: after this introductory section, in the one following (Sec. II) we present an analysis of the results obtained using three models for the CCQE cross sections, while in Sec. III we end by making a few concluding remarks.

II. ANALYSIS OF RESULTS

In this section we discuss the results obtained with the different approaches considered and compare them with the experimental data. Details on the various approaches considered have been presented in previous works. In particular, the SuSA approach and its extension to CC neutrino reactions can be reviewed in [23], whereas the basic ingredients entering in the RMF model applied to inclusive electron and CCQE neutrino reactions are given in [6,7,27,29–31].

We first show results for the CCQE ν_μ-^{12}C double-differential cross section averaged over the neutrino flux $\Phi(E_\nu)$, namely,

$$\frac{d^2\sigma}{dT_\mu d\cos\theta} = \frac{1}{\Phi_{\rm tot}} \int \left[\frac{d^2\sigma}{dT_\mu d\cos\theta}\right]_{E_\nu} \Phi(E_\nu) dE_\nu, \quad (1)$$

where T_μ and θ are the kinetic energy and scattering angle of the outgoing muon, E_ν is the neutrino energy, and $\Phi_{\rm tot}$ is the total flux. For each value of the neutrino energy, the above cross section can be expressed in terms of seven nuclear response functions as [23]

$$\left[\frac{d^2\sigma}{dT_\mu d\cos\theta}\right]_{E_\nu} = \sigma_0 [\hat{V}_{\rm L} R_{\rm L}^{\rm VV} + \hat{V}_{\rm CC} R_{\rm CC}^{\rm AA} + 2\hat{V_{\rm CL}} R_{\rm CL}^{\rm AA} + \hat{V}_{\rm LL} R_{\rm LL}^{\rm AA} + \hat{V}_{\rm T}(R_{\rm T}^{\rm VV} + R_{\rm T}^{\rm AA}) + 2\hat{V}_{\rm T'} R_{\rm T'}^{\rm VA}], \quad (2)$$

where $\hat{V}_i$ are kinematic factors and the indices L, C, T, T′, V, A refer to longitudinal, charge, transverse, transverse-axial, vector, and axial-vector components of the nuclear current, respectively.

In particular, in the SuSA approach each response function can be cast as

$$R_i(q,\omega) = \frac{m_{\rm N}}{q k_{\rm F}} R_i^{\rm sn}(q,\omega) f(\psi), \quad (3)$$

where q and ω are the transferred momentum and energy, respectively, $m_{\rm N}$ is the nucleon mass, $k_{\rm F}$ is the Fermi momentum, $R_i^{\rm sn}$ are the single-nucleon responses, $\psi(q,\omega)$ is the RFG scaling variable (see, e.g. , [21] for its definition), and $f(\psi)$ is the so-called superscaling function, containing the dependence on the nuclear model. In the SuSA model it is given by a fit to the experimental longitudinal (e, e') reduced response function [32].

In the RMF case, the weak response functions are given by taking the appropriate components of the weak hadronic tensor constructed from the single-nucleon current:

$$\langle J_W^\mu \rangle = \int d\mathbf{r} \bar{\phi}_{\rm F}(\mathbf{r}) \hat{J}_W^\mu(\mathbf{r}) \phi_{\rm B}(\mathbf{r}), \quad (4)$$

where $\phi_{\rm B}$ and $\phi_{\rm F}$ are relativistic bound-state and scattering wave functions, respectively, and $\hat{J}_W^\mu$ is the relativistic one-body current operator modeling the coupling between the virtual W and a nucleon [33]. The bound nucleon states are described as self-consistent Dirac-Hartree solutions, derived within an RMF approach by using a Lagrangian containing σ, ω, and ρ mesons [34–36]. The outgoing nucleon wave function is computed by using the same relativistic mean field employed in the initial state. This incorporates the FSI between the ejected nucleon (proton) and the residual nucleus.

Finally, concerning the description of MEC contributions, we use the fully relativistic model of [14,37,38]. In particular, in the $2p$-$2h$ sector we use the scheme applied in[39] to electron scattering, where all many-body diagrams containing two pionic lines were taken into account. However, it is important to point out that, within the present approach, only the pure vector transverse response, $R_{\rm T}^{\rm VV}$, is affected by MEC. Effects in the axial-vector transverse response, as well as the contribution of the correlation diagrams [performed recently for (e, e') in [40]], should be incorporated into the analysis before definitive conclusions on the comparison with data can be drawn. Work along this line is presently under way. MEC contributions to ν-^{12}C reactions have been computed within a somewhat different approach both for charged and neutral currents, in [41,42], where the effect of MEC in the cross section was found to be less than 10%.

In Fig. 1 we show the double-differential cross section averaged over the neutrino energy flux as a function of the muon kinetic energy T_μ. In each panel the results have been averaged over the corresponding angular bin of $\cos\theta$. In all cases we use the standard value of the nucleon axial mass, i.e. , $M_{\rm A} = 1.03$ GeV/c^2. We compare the theoretical results evaluated using the three approaches, SuSA (green line), SuSA + MEC (blue), and RMF (red), with the MiniBooNE data [1]. The case of the most forward angles, $0.9 < \cos\theta < 1$, has not been considered since, as shown in [16], models based on quasifree scattering cannot describe properly this kinematic situation where roughly $1/2$ of the total cross section arises from excitation energies below $\sim$50 MeV.

The analysis of the results corresponding to SuSA and SuSA + MEC approaches and their comparison with data were already presented and discussed at length in [16]. We

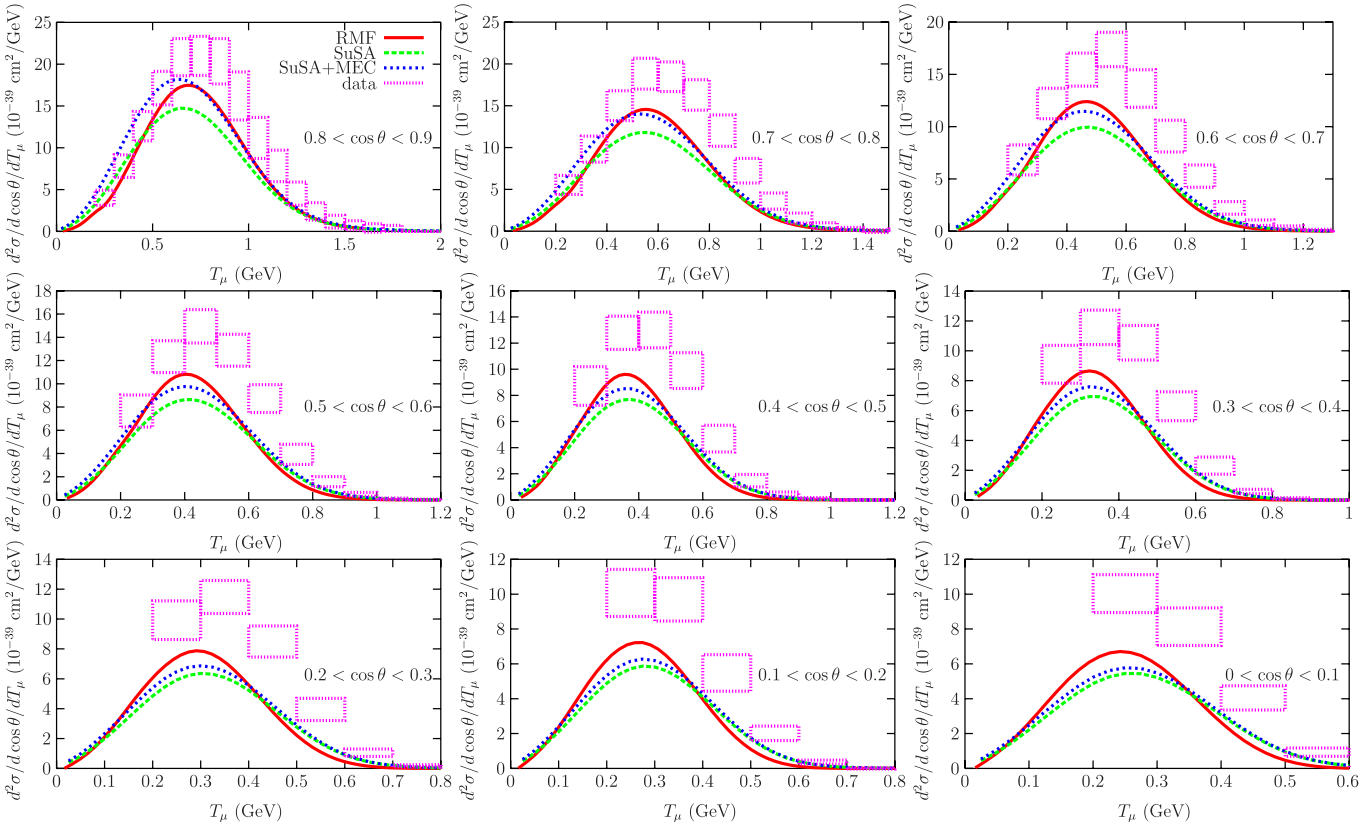

FIG. 1 (color online). Flux-integrated double-differential cross section per target nucleon for the ν_μ CCQE process on ^{12}C evaluated in the SuSA (green line), SuSA + MEC (blue), and RMF (red) models and displayed versus the muon kinetic energy T_μ for various bins of cosθ. The data are from MiniBooNE [1]. The uncertainties do not include the overall normalization error $\delta N = 10.7\%$.

showed that the $2p$-$2h$ MEC increase the cross section, yielding results that are closer to experiment, specifically, for data up to $\cos\theta \sim 0.6$. At larger angles, the discrepancy with experiment becomes larger while, on the other hand, the role of MEC is seen to be less significant, that is, the difference between SuSA and SuSA + MEC becomes smaller as the scattering angle increases.

Cross sections evaluated with the RMF model also yield reasonable agreement with data for smaller angles, the discrepancy becoming larger as θ increases. However, some differences emerge from the comparison between the RMF and SuSA predictions. As observed, RMF cross sections are, in general, larger than the SuSA ones. In particular, in the region close to the peak in the cross section, the RMF result becomes larger than the one obtained with SuSA + MEC. This holds especially for large scattering angles. On the contrary, SuSA and SuSA + MEC get more strength in the region of high muon kinetic energies. This can be attributed to the breakdown of zeroth-kind scaling in the RMF, in contrast to the other approaches where it is assumed to be satisfied. An approach based on RMF, but invoking zeroth-kind scaling, yields results that are much more similar to the SuSA ones.

To make such a statement more transparent, we compare the double-differential cross sections evaluated with the three models, but for fixed values of the scattering angle and muon kinetic energy. The results are presented against the neutrino energy. We have selected as a representative situation the case $\cos\theta = 0.45$ (panel in the middle of Fig. 1) and two values of T_μ: 0.35 GeV that correspond to the maximum in the neutrino-flux-averaged cross section, and $T_\mu = 0.65$ GeV, located in the tail. Results are presented in Fig. 2. As shown, for $T_\mu = 0.35$ GeV (left panel) the three models produce roughly the same response in the maximum at $E_\nu \approx 0.6$ GeV. However, the strength in the tail for higher neutrino energies is much more significant for RMF, being reduced for SuSA + MEC and much smaller for SuSA. This explains why the RMF neutrino-flux-averaged cross section is significantly higher at $T_\mu = 0.35$ GeV (see Fig. 1).

The situation is clearly different for $T_\mu = 0.65$ GeV (right panel in Fig. 2). Here, SuSA and SuSA + MEC cross sections are larger (compared with RMF) even in the region where the cross section reaches its maximum. On the contrary, for larger T_μ (located in the tail), RMF becomes higher. However, notice that for these kinematics the neutrino energies involved are much larger than in the previous case, namely, $E_\nu \geq 0.8$–0.9 GeV; this corresponds to the tail in the experimental neutrino flux whose

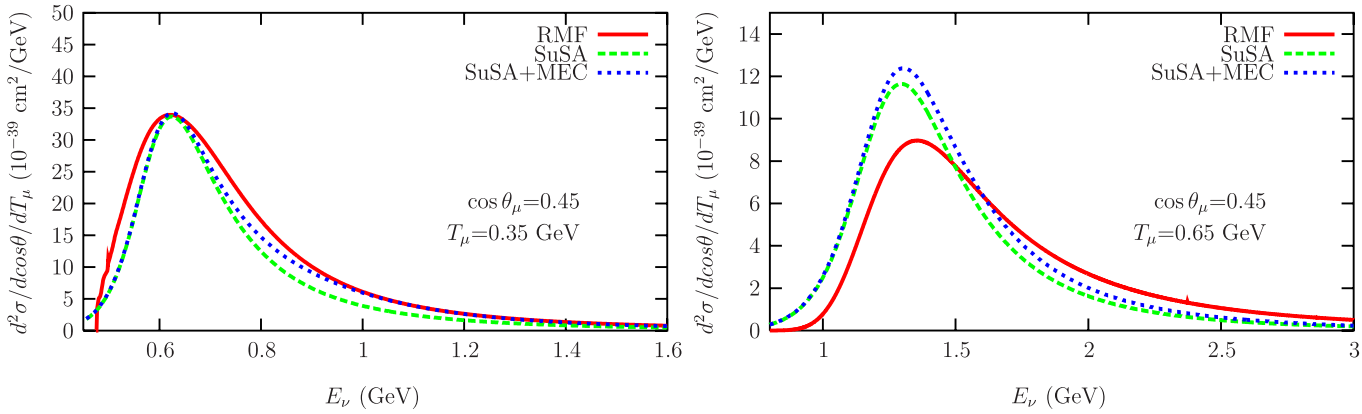

FIG. 2 (color online). Double-differential cross section calculated for fixed values of the muon kinetic energy and scattering angle and displayed versus the neutrino energy. Results presented for the three models: SuSA (green), SuSA + MEC (blue), and RMF (red).

average neutrino energy is 788 MeV. Hence, the main contribution in the averaged cross section comes from the region with smaller values of E_ν where the difference between SuSA (and SuSA + MEC) and RMF is larger. As already mentioned, if one does an RMF calculation that respects zeroth-kind scaling, the results would be essentially in agreement with those of SuSA.

For completeness in Fig. 3 we show the flux-integrated cross section averaged over the bin $0.4 < \cos\theta < 0.5$ evaluated within the framework of the relativistic impulse approximation, but with different descriptions for the FSI. We have considered the relativistic plane wave impulse approximation (RPWIA), that is, switching off FSI in the RMF calculation, and the use of the real part of the relativistic energy-dependent optical potential, denoted as rROP. As already shown in previous works [7,29], these two approaches fulfill scaling, but give rise to scaling functions that lack the asymmetry shown by data. Moreover, scaling of the zeroth kind is also highly respected because of the minor role played in this case by relativistic dynamics in the final state.

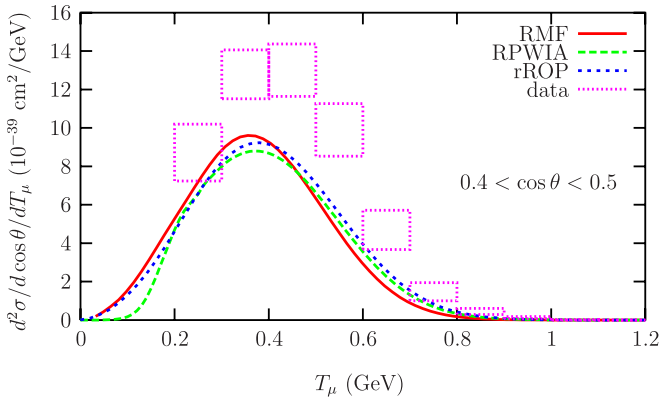

FIG. 3 (color online). As for Fig. 1 for the bin $0.4 < \cos\theta < 0.5$, but now showing the results evaluated with RPWIA (green), rROP (blue), and RMF (red).

Results in Fig. 3 show that the RPWIA and rROP approaches are very similar for all T_μ values, being also in accordance with RMF, although here the maximum in the cross section is slightly reduced while strength is shifted to larger values of the muon kinetic energy. This is a consequence of the differences introduced in the scaling functions by the particular description of FSI and its impact on the relativistic nuclear dynamics and the isospin (third-kind) and zeroth-kind scaling violations [27].

In Fig. 4 we plot the neutrino-flux-averaged cross section versus the scattering angle at fixed T_μ (averaged over each bin). For low muon momenta the three models tend to underestimate the data, improving the agreement as T_μ increases. As observed, when added to the SuSA results, the $2p$-$2h$ MEC yields an enhancement of the cross section whose magnitude increases for more forward scattering angles. This result holds for each bin in T_μ. With respect to comparison with data, some general comments already made for the SuSA and SuSA + MEC results [16] also apply to RMF: the last also underestimates the data at large muon scattering angles, particularly for small T_μ. However, some important differences between RMF and SuSA-based models also emerge. Let us comment on the general trend followed by the RMF results as functions of $\cos\theta$ that clearly differ from SuSA and SuSA + MEC. In the six panels presented in Fig. 4 RMF cross sections are the lowest for the smallest values of $\cos\theta$. As we move to more positive $\cos\theta$, the RMF cross section grows faster, lying above the results corresponding to SuSA + MEC in the intermediate region. Finally, for smaller values of the scattering angle, namely, $\cos\theta$ approaching 0.9, while RMF inverts its behavior and decreases very rapidly, SuSA and SuSA + MEC approaches to $\cos\theta = 0.9$ show a much softer slope. In fact, this is the region where the discrepancy between RMF and SuSA-based models can be better appreciated. It is very illustrative to point out that the general shape presented by the RMF cross section as a function of $\cos\theta$ fits perfectly well the shape shown by data, although RMF predictions fall below the data for

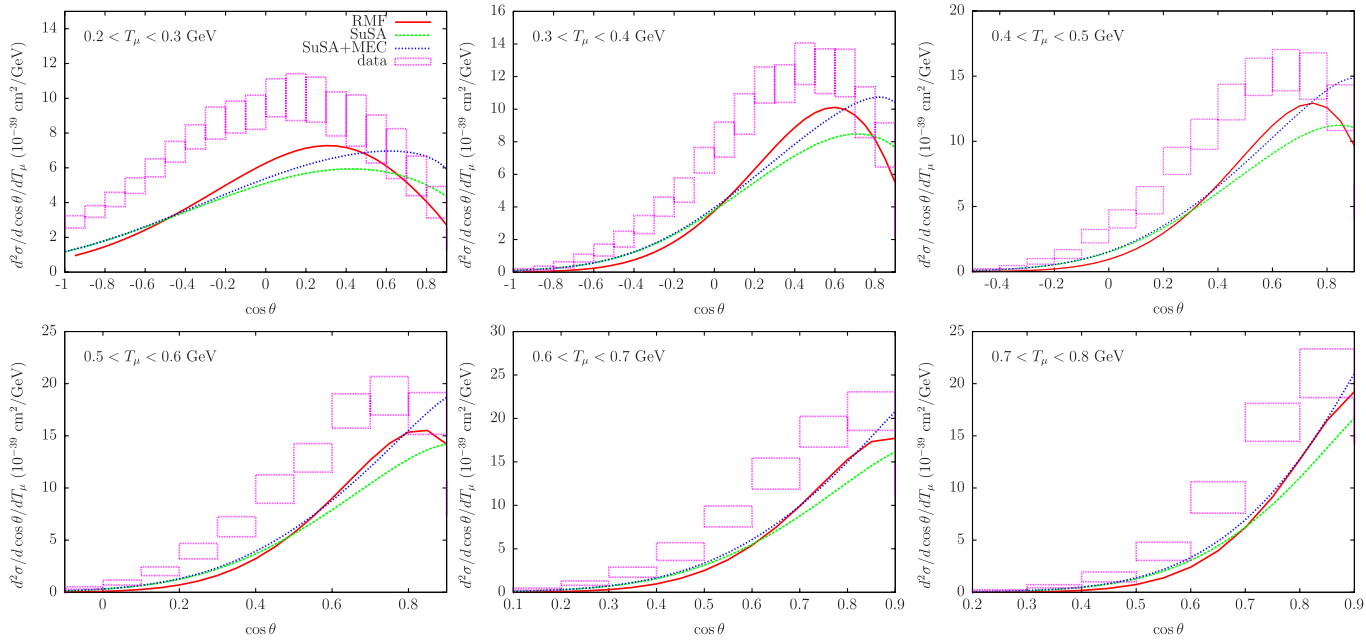

FIG. 4 (color online). Double-differential ν_μ CCQE cross section for ^{12}C integrated over neutrino flux versus the outgoing muon scattering angle for various bins of the muon kinetic energy T_μ. Results are given for RMF (red lines), SuSA (green), and SuSA + MEC (blue).

small muon momenta. The different behavior of the models is partly due to the fact that the RMF is better describing the low-energy excitation region whereas, as already pointed out, the SuSA model has no predictive power at very low angles, where the cross section is dominated by low excitation energies and the superscaling ideas are not supposed to apply. For this reason we do not show results for the highest cosθ bin.

In Fig. 5 we present the results obtained by integrating the flux-averaged double-differential cross sections over cosθ (upper panel) and T_μ (bottom panel), respectively. In addition to the three models considered in previous graphs, here we also include for reference the predictions given by the RFG. It is interesting to remark that, in spite of the clear differences shown by the RMF and SuSA predictions for the double-differential cross sections (Figs. 1 and 4), the integrated results almost coincide. On the contrary, the $2p$-$2h$ MEC effects produce a visible enhancement in the cross section that is closer to the experimental data. The RFG results lie somewhere between the SuSA/RMF and SuSA + MEC predictions.

To conclude this section, in Fig. 6 we display the total QE cross section per neutron obtained in the models discussed above as a function of the neutrino energy and compared with the experimental data. Note that here the integration is performed over all muon scattering angles ($-1 < \cos\theta < 1$) and energies ($0 < T_\mu < E_\nu$).

As observed in Fig. 5, the discrepancies between the various models tend to be washed out by the integration, yielding very similar results for the models that include FSI (SuSA, RMF and rROP), all of them giving a lower total cross section than the models without FSI (RFG and RPWIA). We remind the reader that here the standard value $M_A = 1.03$ GeV$/c^2$ is used. A larger "effective" axial mass $1.35 < M_A^{\text{eff}} < 1.65$ GeV$/c^2$ would yield results for the RMF and SuSA models compatible with the MiniBooNE data.

On the other hand, the SuSA + MEC curve, while being closer to the data at high neutrino energies, has a somewhat different shape with respect to the other models, in qualitative agreement with the relativistic calculation of [15]. It should be noted, however, that the result is affected by an uncertainty of about 5% associated with the treatment of the $2p$-$2h$ contribution at low momentum transfers.

III. CONCLUDING REMARKS

Summarizing, in this paper we extend the previous work presented in [16] where the focus was placed on the use of the phenomenological SuSA model and its extension incorporating the role played by $2p$-$2h$ MEC contributions. Here, our main interest resides in the predictions provided by the RMF approach. This model has been successfully applied to inclusive QE (e, e') processes where it has been shown to be capable of reproducing the specific asymmetric shape shown by the experimental scaling function. On the other hand, and unlike the SuSA approach which assumes scaling of the zeroth kind, i.e. , equal longitudinal and transverse scaling functions, the RMF provides a transverse scaling function that exceeds by about $\sim$20% the longitudinal one. This result seems to be in accordance

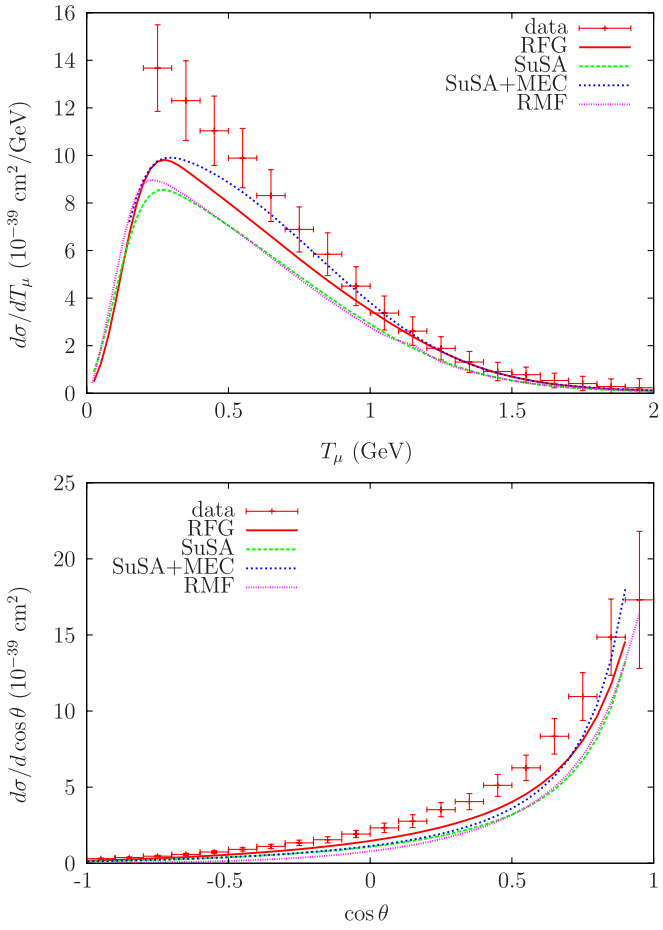

FIG. 5 (color online). Results obtained with SuSA, SuSA + MEC, RMF, and RFG models. Upper panel: Flux-averaged integrated cross section displayed versus the muon kinetic energy. Bottom panel: As for the upper one, but now for the flux-averaged muon angular distribution.

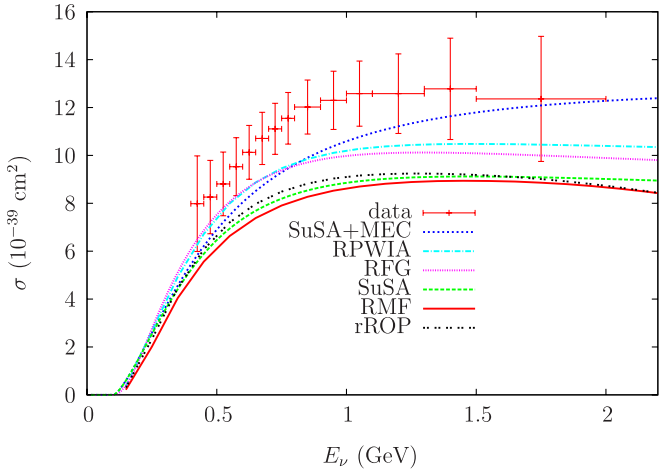

FIG. 6 (color online). Total CCQE cross section per neutron versus the neutrino energy. The curves corresponding to different nuclear models (see text) are compared with the flux unfolded MiniBooNE data [1].

with the most recent analyses of the L/T separated (e, e') data. Thus, this violation of scaling of the zeroth kind has visible effects when proceeding to studies of CCQE cross sections. Furthermore, the different isospin content (namely, violations of third-kind scaling) of the electromagnetic and CC weak nucleon form factors should also be carefully considered [27].

In this work we apply the RMF model to CCQE neutrino reactions on ^{12}C corresponding to the kinematics of the MiniBooNE experiment. Results for the flux-averaged double-differential cross sections are compared with data and the predictions given by SuSA and SuSA + MEC models. Generally speaking, the RMF model underestimates the data especially at large muon scattering angles and low muon energies. This was already observed with SuSA and to a somewhat lesser extent with SuSA + MEC. However, the specific behavior shown by RMF clearly differs from that of SuSA and SuSA + MEC; the maximum in $d^2\sigma/d\cos\theta dT_\mu$ as a function of T_μ for various bins of $\cos\theta$ gets higher for RMF, whereas the tail at high T_μ is more pronounced for the SuSA-based models. Also, the general trend shown by the curve corresponding to the double-differential cross section as a function of the scattering angle for bins of T_μ clearly differs for RMF and SuSA (SuSA + MEC) approaches. Here, it is very interesting to point out that the specific shape followed by RMF predictions fits perfectly well the slope shown by data.

The single-differential cross sections shown in Fig. 5 where the three calculations yield very similar predictions, with almost the same shape and underpredicting the data, also show that it is very useful to compare double-differential cross sections as in Fig. 4, where differences among models may be more easily seen.

To conclude, let us note that, in spite of the discrepancies introduced by the models in the double-differential cross sections, RMF and SuSA approaches provide almost identical results for the single-differential cross section, this being found to lie below the data. Although the inclusion of $2p$-$2h$ MEC contributions increases the differential cross section without a significant change of the shape, and thus seems to improve the agreement with the data as shown in Figs. 2 and 5, it is also seen (in Fig. 2, but more clearly in Fig. 4) that the shape of the cross section is best reproduced by the RMF and does not improve with the inclusion of the $2p$-$2h$ MEC contributions in SuSA. It is tempting to hypothesize that the addition of the $2p$-$2h$ MEC effects to the RMF results would lead to reasonable agreement in both magnitude and shape with the experimental double-differential cross section.

Finally, as shown in Fig. 6, the impact of the $2p$-$2h$ contribution on the total cross section increases with the neutrino energy, suggesting that the data can be explained without the need for a large nucleon axial mass. However, more refined calculations taking care of correlation currents, MEC effects in the axial-vector channel, etc.,

should be performed before definitive conclusions can be drawn.

ACKNOWLEDGMENTS

This work was partially supported by DGI (Spain): FIS2008-01143, FPA2010-1742, FIS2008-04189, by the Junta de Andalucía, by the INFN-MEC Collaboration agreement, projects FPA2008-03770-E-INFN, ACI2009-1053, the Spanish Consolider-Ingenio 2000 programmed CPAN (CSD2007-00042), and partially (T. W. D) by the U.S. Department of Energy under cooperative agreement DE-FC02-94ER40818.

[1] A. A. Aguilar-Arevalo *et al.* (MiniBooNE Collaboration), Phys. Rev. D **81**, 092005 (2010).
[2] V. Bernard, L. Elouadrhiri, and U. G. Meissner, J. Phys. G **28**, R1 (2002).
[3] M. B. Barbaro, A. De Pace, T. W. Donnelly, A. Molinari, and M. J. Musolf, Phys. Rev. C **54**, 1954 (1996).
[4] O. Benhar, P. Coletti, and D. Meloni, Phys. Rev. Lett. **105**, 132301 (2010).
[5] C. Juszczak, J. T. Sobczyk, and J. Zmuda, Phys. Rev. C **82**, 045502 (2010).
[6] C. Maieron, M. C. Martinez, J. A. Caballero, and J. M. Udias, Phys. Rev. C **68**, 048501 (2003).
[7] J. A. Caballero, Phys. Rev. C **74**, 015502 (2006).
[8] J. E. Amaro, M. B. Barbaro, J. A. Caballero, T. W. Donnelly, and J. M. Udias, Phys. Rev. C **75**, 034613 (2007).
[9] J. A. Caballero, M. C. Martinez, J. L. Herraiz, and J. M. Udias, Phys. Lett. B **688**, 250 (2010).
[10] A. Meucci, J. A. Caballero, C. Giusti, F. D. Pacati, and J. M. Udias, Phys. Rev. C **80**, 024605 (2009).
[11] M. Martini, M. Ericson, G. Chanfray, and J. Marteau, Phys. Rev. C **80**, 065501 (2009).
[12] M. Martini, M. Ericson, G. Chanfray, and J. Marteau, Phys. Rev. C **81**, 045502 (2010).
[13] J. E. Amaro, M. B. Barbaro, J. A. Caballero, T. W. Donnelly, and A. Molinari, Nucl. Phys. **A643**, 349 (1998).
[14] J. E. Amaro, M. B. Barbaro, J. A. Caballero, T. W. Donnelly, and A. Molinari, Phys. Rep. **368**, 317 (2002).
[15] J. Nieves, I. Ruiz Simo, M. J. Vicente Vacas, Phys. Rev. C **83**, 045501 (2011).
[16] J. E. Amaro, M. B. Barbaro, J. A. Caballero, T. W. Donnelly, and C. F. Williamson, Phys. Lett. B **696**, 151 (2011).
[17] D. B. Day, J. S. McCarthy, T. W. Donnelly, and I. Sick, Annu. Rev. Nucl. Part. Sci. **40**, 357 (1990).
[18] T. W. Donnelly and I. Sick, Phys. Rev. Lett. **82**, 3212 (1999).
[19] T. W. Donnelly and I. Sick, Phys. Rev. C **60**, 065502 (1999).
[20] C. Maieron, T. W. Donnelly, and I. Sick, Phys. Rev. C **65**, 025502 (2002).
[21] W. M. Alberico, A. Molinari, T. W. Donnelly, E. L. Kronenberg, and J. W. Van Orden, Phys. Rev. C **38**, 1801 (1988).
[22] J. E. Amaro, M. B. Barbaro, J. A. Caballero, T. W. Donnelly, and C. Maieron, Phys. Rev. C **71**, 065501 (2005).
[23] J. E. Amaro, M. B. Barbaro, J. A. Caballero, T. W. Donnelly, A. Molinari, and I. Sick, Phys. Rev. C **71**, 015501 (2005).
[24] J. R. Vignote, M. C. Martinez, J. A. Caballero, E. Moya de Guerra, and J. M. Udias, Phys. Rev. C **70**, 044608 (2004).
[25] J. M. Udias, P. Sarriguren, E. Moya de Guerra, E. Garrido, and J. A. Caballero, Phys. Rev. C **51**, 3246 (1995).
[26] T. W. Donnelly and C. F. Williamson (private communication).
[27] J. A. Caballero, J. E. Amaro, M. B. Barbaro, T. W. Donnelly, and J. M. Udias, Phys. Lett. B **653**, 366 (2007).
[28] M. C. Martinez, P. Lava, N. Jachowicz, J. Ryckebusch, K. Vantournhout, and J. M. Udias, Phys. Rev. C **73**, 024607 (2006).
[29] J. A. Caballero, J. E. Amaro, M. B. Barbaro, T. W. Donnelly, C. Maieron, and J. M. Udias, Phys. Rev. Lett. **95**, 252502 (2005).
[30] J. E. Amaro, M. B. Barbaro, J. A. Caballero, and T. W. Donnelly, Phys. Rev. Lett. **98**, 242501 (2007).
[31] J. L. Herraiz, M. C. Martinez, J. M. Udias, and J. A. Caballero, Acta Phys. Pol. B **40**, 2405 (2009).
[32] J. Jourdan, Nucl. Phys. **A603**, 117 (1996).
[33] J. M. Udias, P. Sarriguren, E. Moya de Guerra, E. Garrido, and J. A. Caballero, Phys. Rev. C **48**, 2731 (1993); **51**, 3246 (1995).
[34] C. J. Horowitz and B. D. Serot, Nucl. Phys. **A368**, 503 (1981); Phys. Lett. **86B**, 146 (1979).
[35] B. D. Serot and J. D. Walecka, *Advances in Nuclear Physics* edited by J. W. Negele, E. W. Vogt (Plenum Press, New York, 1986), Vol. 16, p. 1.
[36] M. M. Sharma, M. A. Nagarajan, and P. Ring, Phys. Lett. B **312**, 377 (1993).
[37] J. E. Amaro, M. B. Barbaro, J. A. Caballero, T. W. Donnelly, and A. Molinari, Nucl. Phys. **A723**, 181 (2003).
[38] J. E. Amaro, M. B. Barbaro, J. A. Caballero, T. W. Donnelly, C. Maieron, and J. M. Udias, Phys. Rev. C **81**, 014606 (2010).
[39] A. De Pace, M. Nardi, W. M. Alberico, T. W. Donnelly, and A. Molinari, Nucl. Phys. **A726**, 303 (2003).
[40] J. E. Amaro, C. Maieron, M. B. Barbaro, J. A. Caballero, and T. W. Donnelly, Phys. Rev. C **82**, 044601 (2010).
[41] Y. Umino and J. M. Udias, Phys. Rev. C **52**, 3399 (1995).
[42] Y. Umino, J. M. Udias, and P. J. Mulders, Phys. Rev. Lett. **74**, 4993 (1995).